RESEARCH REPORTS

STRESS ANALYSIS IN TWO DIMENSIONAL BENDING PROCESS USING THE PHOTO-RHEOLOGICAL STRESS ANALYSIS

Yoshio OHASHI and Tadashi NISHITANI

Department of Mechanical Engineering

(Received September, 11, 1971)

1. Introduction

Bending process is one of the important processes in plastic working, and there are many investigations in the stress analysis concerning this process[1)-3)]. However, as there was no method to observe directly the stress states within tool and work piece during plastic working, the method of stress analysis still remains of comparatively low accuracy based on some simple assumptions.

Generally, contact problems between elastic tool and plastically flowing work piece arise in the plastic works. Especially, as the stress states within the bodies near the contact surface are affected seriously not only by the mechanical properties of bodies in contact but also by the friction determined with the roughness and lubrication on the surface, the states will be of unexpectedly complicated.

Therefore, it seems to be natural that the problems concerning the friction and lubrication on the contact surface have attracted attention of many investigators in the field of plastic works and many investigations have been performed in this respect[4)5)]. However, since the experimental observation has been confined in the measurement of indirect or synthetic amount instead of direct measurement of stress state appearing actually on the contact surface, it seems inevitable that these investigations are confined within some limits. If the direct observation of the stress states during processing would be possible, further progress may be expected to improve the plastic working as the result of stress analysis with higher accuracy.

The stress state and its time dependent variation in the plastically flowing bodies may be measured with the same accuracy as in the photoelasticity by means of the photo-rheological stress analysis[6)10)] proposed by one of the present authors. Accordingly, the present authors have clarified the stress states and their time dependent variations in the vicinity of contact surface for the contact problems between elastic and plastically flowing bodies by means of the combination of the photo-elasticity and pheto-rheological stress analysis[7)-10)].

In the present paper, these methods are applied to the two dimensional bending process in the plane strain state, and the stress states within tool and work

piece as well as on their contact surface are investigated in detail during processing. As this method is related to a model test and the problem is considered in the plane strain state, the result obtained by this method is not always valuable as the direct reference for actual bending process of metallic material. However, as the deformation mode can be easily magnified in the model test, the model test is rather preferable for considering the element to be taken into account in the analysis. Furthermore, the result herein obtained has a possibility to be used as a direct reference for metal under some corrersponding ranges.

2. Experimental apparatus and specimens

The experimental apparatus is the same as in the previous paper[3)-10)]. The experiment was performed with specimens shown in Fig. 1 in an oil bath heated at 65°C. The celluloid strip is restrained by the two thick glass plates on both surfaces of it in order to restrict the deformation of strip in the plane strain state. Moreover, the errors of temperature distribution in the deforming part of specimen and its variation during the bending process are kept within ± 0.05°C by means of the regulator of thermistor type.

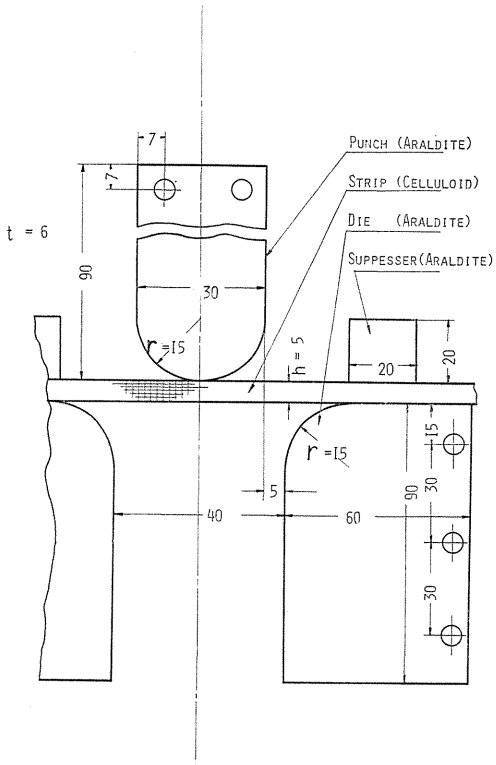

FIG. 1. Geometries of specimens.

The specimens of punch, die and suppresser were finished smoothly, especially on the contact surface, with end-milling from an araldite plate without initial stress.

To investigate the stress state in the strip with high accuracy, it is preferable to select the thickness of strip h as thick as possible in the range allowed by the apparatus. Therefore, the thickness h was selected as $h=5$ mm in considering the value of $r/h=3$, which is almost in the limit of its usnal range, where r denotes the contour radii of punch and die.

As the result of calibration test using two uniaxial specimens cut out from the same araldite plate as above, the material was confirmed to remain in its glassy elastic state at 65°C. Young's modulus and fringe stress of araldite at 65°C were found as 234 kg/mm^2 and 0.96 kg/mm, respectively.

The strip was finished by end-milling from the transparent celluloid plate of 6 mm thick, and its contact surfaces were extremely smooth. For tracing the location and deformation state of the assigned element during deformation, the network with spaces of 1 mm and 0.5 mm in the tangential and thickness directions was incised on one side of it.

The calibration test of the celluloid strip was performed with uniaxial specimens under a combined loading of uniaxial tensile stress σ_1 and hydrostatic pressure σ_2. The fundamental relations in the photo-rheological stress analysis[6)10)] used in the above mentioned calibration test are as follows;

i) loading process

$$\Delta\varepsilon_p(t)=\frac{2}{3}B_0\int_0^t\tau^{\alpha}\Delta\sigma(\tau)e^{\frac{b}{\sqrt{3}}\Delta\sigma(\tau)}d\tau+\frac{\Delta\sigma(t)}{2G}\left\{\frac{\Delta\sigma(t)}{\sqrt{3}\,k}\right\}^{2n}, \tag{1}$$

$$N(t)=C_1\Delta\sigma(t)+C_2\Delta\varepsilon_p(t)+C_3\left\{\Delta\varepsilon_p(t)\right\}^{3/2}+C_4\left\{\Delta\varepsilon_p(t)\right\}^{2}, \tag{2}$$

ii) unloading process

$$\Delta\bar{\varepsilon}_p(t)=\frac{2}{3}B_1\int_{t*}^t(\tau-t^*)^{\beta}\Delta\bar{\sigma}(\tau)e^{\frac{b'}{\sqrt{3}}\Delta\bar{\sigma}(\tau)}d\tau-\frac{2}{3}B_0'\int_{t*}^t\tau^{\alpha}\Delta\sigma(\tau)e^{\frac{b}{\sqrt{3}}\Delta\sigma(\tau)}d\tau, \tag{3}$$

$$\bar{N}(t)=C_5\Delta\bar{\sigma}(t)+C_6\Delta\bar{\varepsilon}_p(t), \tag{4}$$

where $\Delta\sigma(t)$ and $\Delta\varepsilon_p(t)$ denote the principal stress and plastic-strain differences at the instant of time t, $N(t)$ is the fringe order at the same instant, t_* shows the time t at the beginning of unloading, and $\Delta\bar{\sigma}(t)=\Delta\sigma(t)-\Delta\sigma(t_*)$, $\Delta\bar{\varepsilon}_p(t)=\Delta\varepsilon_p(t)-\Delta\varepsilon_p(t_*)$, $\bar{N}(t)=N(t)-N(t_*)$. The symbols B_0, α, b, $\cdots$, C_5 and C_6 denote the characteristic values depending on the material, temperature and others found from the above mentioned calibration test. As the characteristic values in eqs. (1) and (3) are affected by the principal stress ratio σ_1/σ_2, the calibration test was performed for several values of it. The relations between $\Delta\sigma$ and $\Delta\varepsilon$ in the loading process in relation to the value of σ_1/σ_2 (or σ_2/σ_1) are

TABLE 1. Characteristic values ($\sigma_2/\sigma_1=0$)

B	$-\alpha$	b	$2G$	k	n	B'_0	$2G'$	$-\beta$
3.75×10^{-4}	0.426	6.74	59.0	0.86	2.23	0.25×10^{-4}	132	0.514
b'	B_1	C_1	C_2	C_3	C_4	C_5	C_6	
5.94	1.3×10^{-4}	0.22	1.6	0.2	0.1	0.16	1.3	

shown in Fig. 2, for example. As an example, the characteristic values for $\sigma_1/\sigma_2=0$ is shown in Table 1.

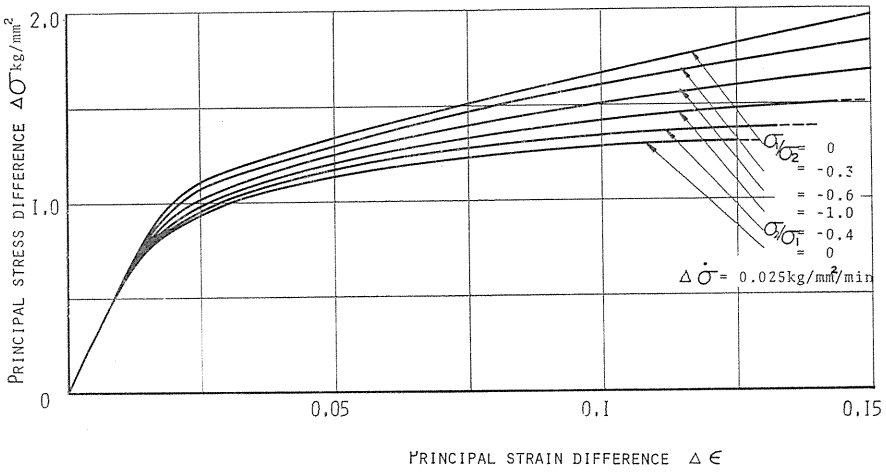

FIG. 2. Relation between $\Delta\sigma$ and $\Delta\varepsilon$ in the loading process.

3. Experimental procedure and its result

In the above mentioned apparatus, after the temperature was settled at 65°C, a dead load 18 kg was applied instantly, and the isochromatic and isoclinic patterns as well as the patterns of deformed network at the instants of $t=2$, 30, 90 and 180 min after loading were photographed in order to trace the stress and deformation states of each element within the specimens.

In these cases, as the specimens are in the oil bath filled with spindle oil, it can be considered that the contact surface would be lubricated sufficiently.

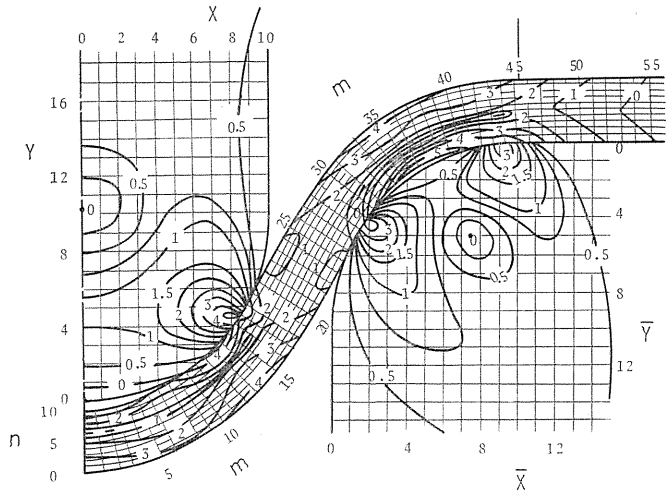

FIG. 3. Isochromatic pattern at 2 min after loading.

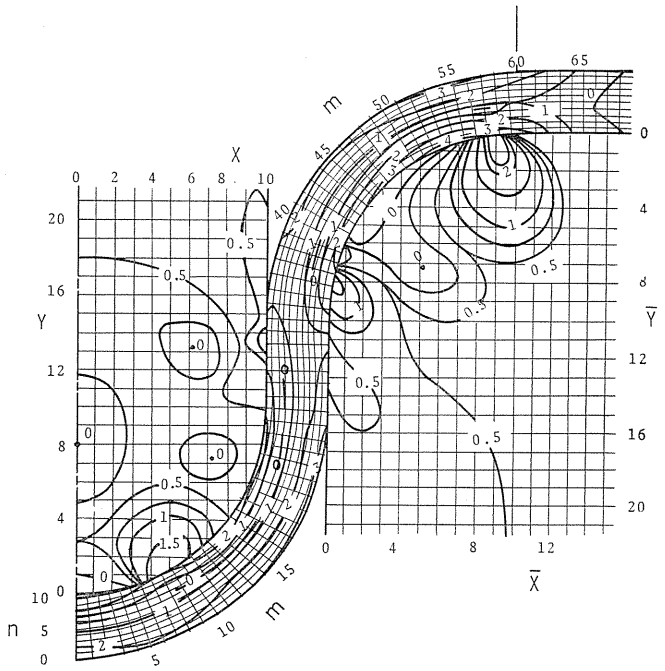

FIG. 4. Isochromatic pattern at 180 min after loading.

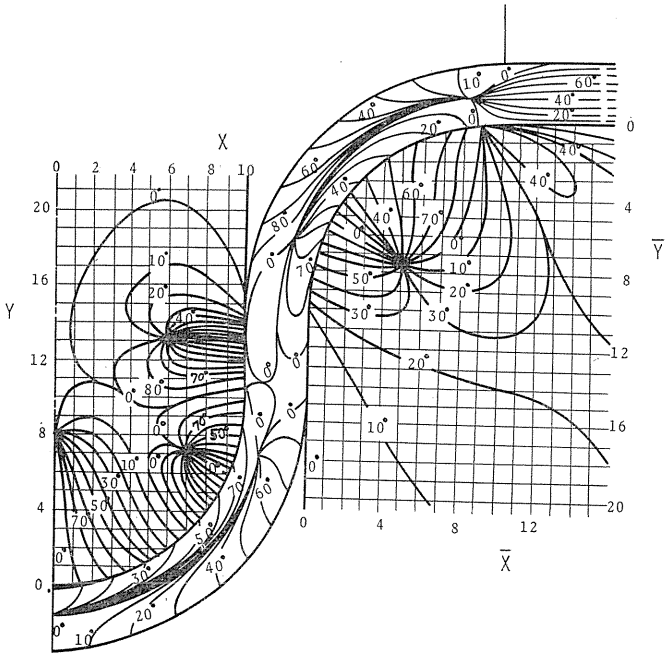

Fig. 5. Isoclinic pattern at 180 min after loading.

As examples of the results obtained, Figs. 3 and 4 show the isochromatic patterns at 2 and 180 min after loading. Fig. 5 shows the isoclinic pattern at 180 min after loading. In the specimens of punch and die, it was difficult to obtain the patterns having the sufficient densities for analysing the stress states by means of the usual method. Then, the isochromatic patterns having the quarter orders were obtained by using the fringe multiplication method[11] by means of the duplicate printing of isochromatics in the dark and bright fields. The symbols m and n entered in the strip in Figs. 3 and 4 denote the order of lines in the network after deformation. As the fringe pattern in the suppresser was of the low order inadequate for analysis, the stress state in it has not been analysed.

4. Stress distributions in the specimens

4.1. Stress distributions in the punch and die

As the punch and die specimens are in their elastic states, the stress states may be analysed by the usual shear difference method from the isochromatic patterns in Figs. 3 and 4 and the isoclinic pattern in Fig. 5, for example. As shown in Figs. 3 and 5, Sections $X=0, 1, \ldots, 10$ divide the half width of punch equally, and Sections $Y=0, 1, 2, \ldots$ are entered with the same spacing as above. Sections $\overline{X}=0, 1, 2, \ldots$ and $\overline{Y}=0, 1, 2, \ldots$ are also entered with the same spacing on the die, as shown in Figs. 3 to 5.

As an example, the stress distributions on Sections $Y=12$, 6 and 2 in the punch at 180 min afaer loading are shown in Fig. 6. Fig. 7 shows them on Sections $\overline{Y}=12$, 6 and 2 in the die at 180 min after loading.

4.2. Stress distribution in the strip

Since the strip flows plastically, the following relations (5) and (6) for plane strain state corresponding to the relations (1) and (3) in the calibration test as well as the relations (2) and (4) should be considered for obtaining the principal stress difference $\Delta\sigma$ of each element in relation to time by means of the photorheological stress analysis:

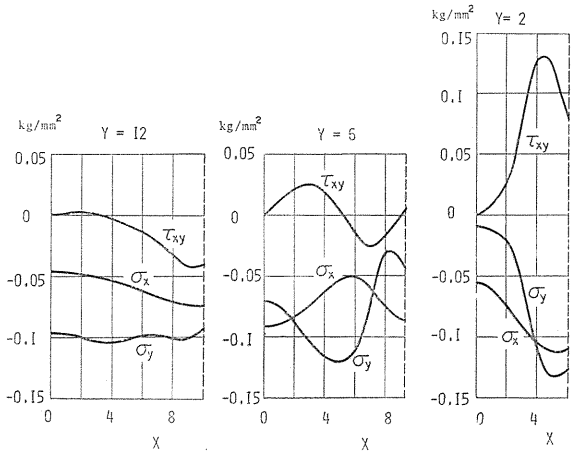

FIG. 6. Stress distributions in the punch at 180 min after loading.

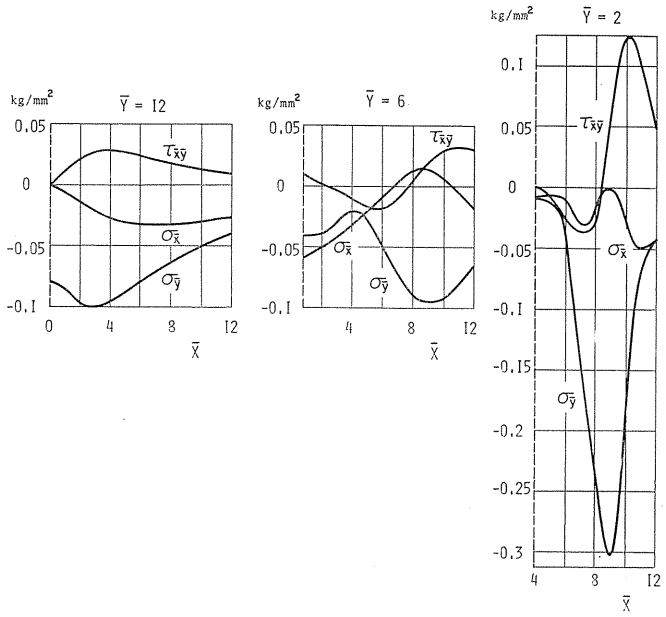

FIG. 7. Stress distributions in the die at 180 min after loading.

i) loading process

$$\Delta\dot{\bar{\varepsilon}}_p(t) = \frac{B_0}{2} t^{\alpha} \Delta\sigma(t) e^{\frac{b}{2}\Delta\sigma(t)} + (2n+1)\frac{\Delta\dot{\sigma}(t)}{2G}\left\{\frac{\Delta\sigma(t)}{2k}\right\}^{2n}, \tag{5}$$

ii) unloading process

$$\Delta\dot{\bar{\varepsilon}}_p(t-t_*) = \frac{B_1}{2}(t-t_*)^{\beta}\Delta\bar{\sigma}(t) e^{\frac{b'}{2}\Delta\bar{\sigma}(t)} - \frac{B_0'}{2} t^{\alpha}\Delta\sigma(t) e^{\frac{b}{2}\Delta\sigma(t)}. \tag{6}$$

Calculation procedures using these relations are described in the previous paper[6) 10)].

As the coefficients in eq. (5) are affected by the value of σ_1/σ_2, it is necessary to consider the effect of σ_1/σ_2 on these coefficients, for improving the accuracy of stress analysis. However, the value of σ_1/σ_2 varies with time and location and is not known beforehand. Accordingly, as the first approximation, the value of $\Delta\sigma$ was evaluated by using the values of coefficients shown in Table 1 for $\sigma_2/\sigma_1 = 0$. The stress components in each point were found from the distribution of $\Delta\sigma$ herein obtained and the isoclinic pattern in Fig. 5, for example.

The values of σ_2/σ_1 thus obtained are shown in Fig. 8 in relation to time at several elements on the die side in the strip. As it was very laborious and time consuming to take into account the time dependent variation of σ_2/σ_1 in the analysis exactly, an effective approximation was employed. That is, the time was devided into three intervals 0~30, 30~90 and 90~180 min, and the mean value of σ_2/σ_1 in each interval was considered. They are shown in Fig. 8 with the dashed lines for the element $m=25$, $n=2$. The values of coefficients corresponding to

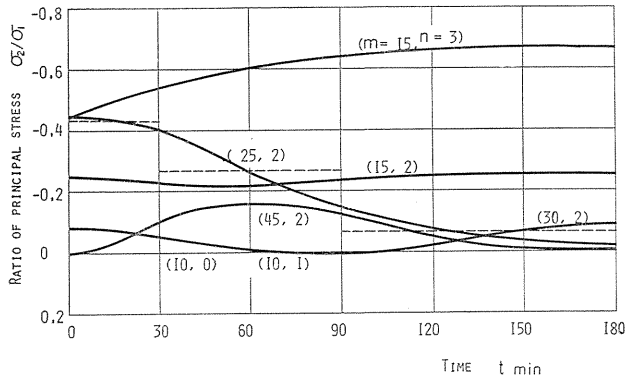

FIG. 8. Relation between principal stress ratio and time.

these three values of σ_2/σ_1 were used for eq. (5) in accordance with the above mentioned time intervals, for obtaining the values of $\Delta\sigma$. By way of precaution, the result of this method was compared with that obtained by the method in which the variation of σ_2/σ_1 was taken into account exactly, on the element having the largest time dependent variation of σ_2/σ_1 ($m=25$, $n=2$ in Fig. 8). As the result of this comparison, it was confirmed that the maximum difference between

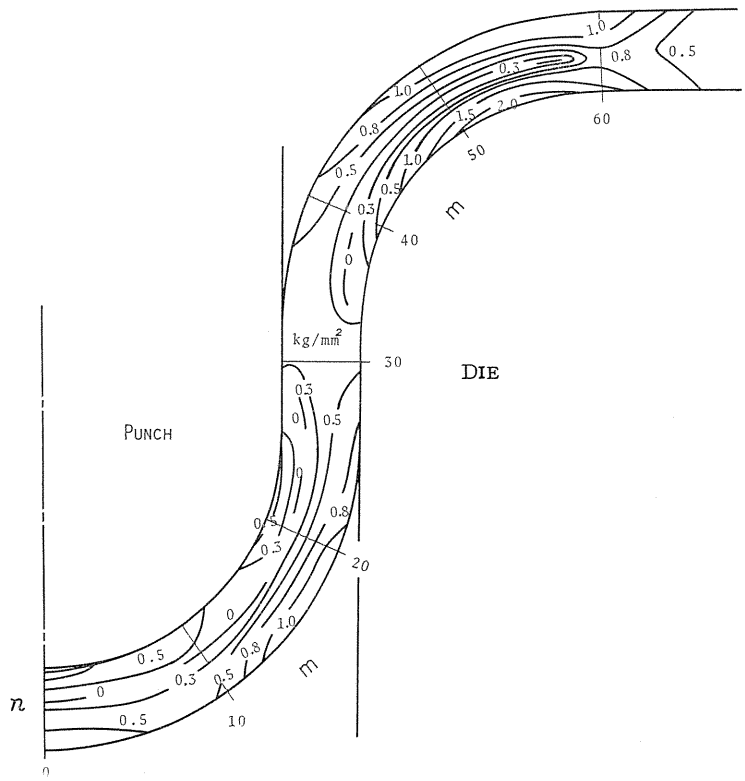

FIG. 9. Distributions of $\Delta\sigma$ (kg/mm²) in the strip at 180 min after loading.

them lay within 5 percent. Therefore, the above mentioned approximate method was employed for every point.

Though some elements in the tension side of the bent strip may be in the plane stress state, the maximum error of $\Delta\sigma$ between those calculated in the plane

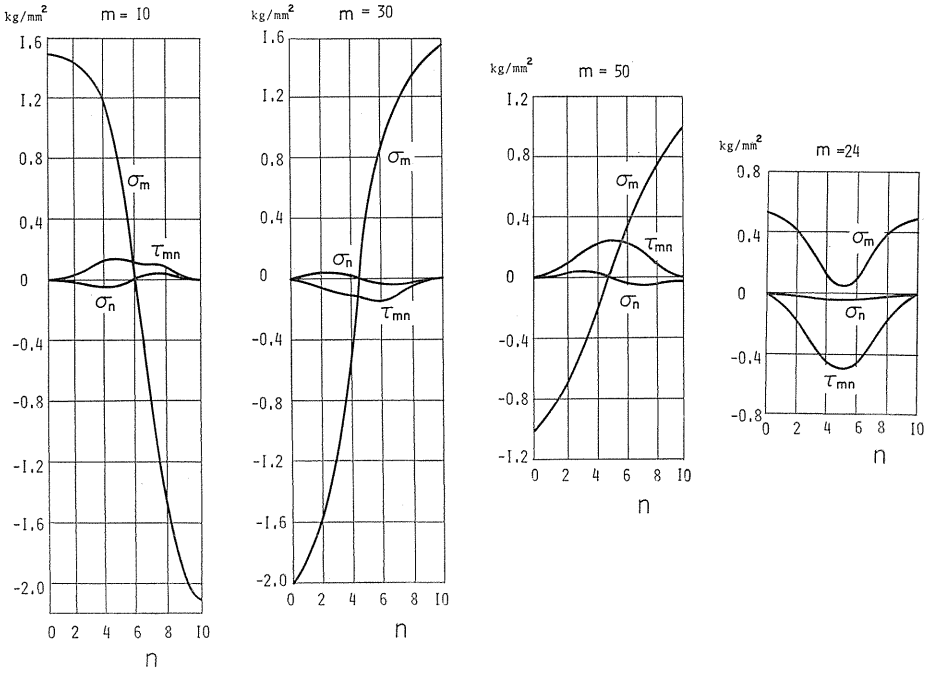

FIG. 10. Stress distributions in the strip at 2 min after loading.

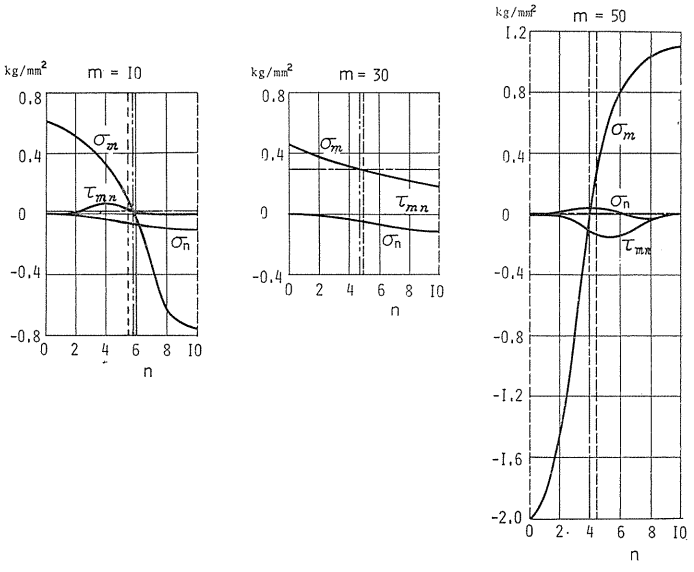

FIG. 11. Stress distributions in the strip at 180 min after loaging.

stress and in the plane strain state was ascertained to be negligibly small of within 1.5 percent. Accordingly, in this paper, the value of $\Delta\sigma$ in each element of the strip was evalueted in the plane strain state.

As an example of the results thus obtained, Fig. 9 shows the distribution of $\Delta\sigma$ in the strip at 180 min after loading. The stress distribution in the strip was obtained by the shear difference method from the distribution of $\Delta\sigma$ and the isoclinic pattern. As examples, the stress distributions in Sections $m=10$, 30 and 50 at 2 and 180 min after loading are shown in Figs. 10 and 11.

5. Stress distribution on the contact surface

Figs. 12 and 13 show the distributions of normal stress components σ_m and σ_n in the tangential and thickness directions on the contact surface of strip at 2

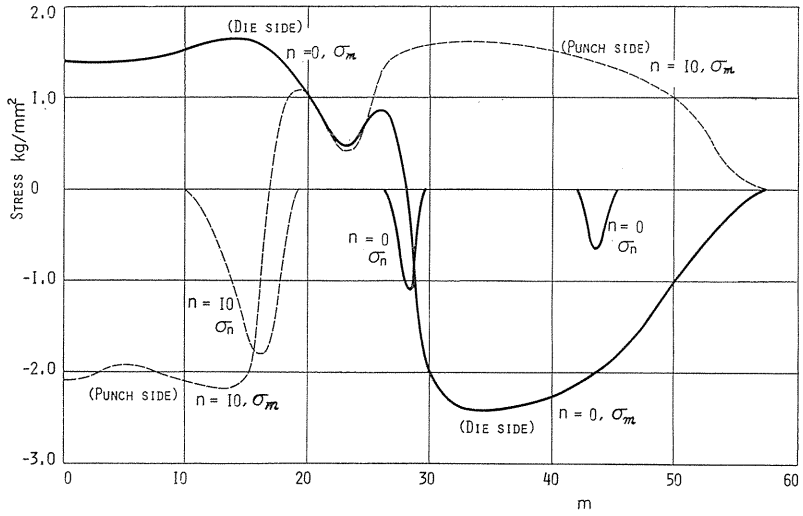

FIG. 12. Stress distributions on the contact surface at 2 min after loading.

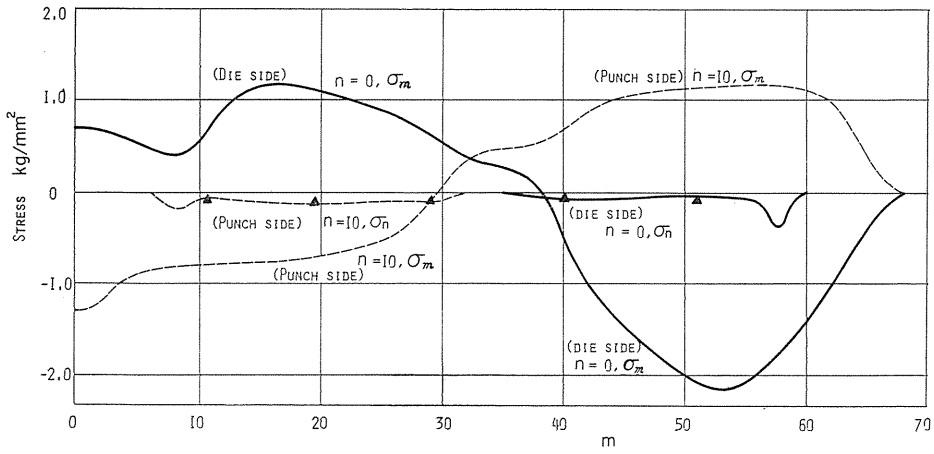

FIG. 13. Stress distributions on the contact surface at 180 min after loading.

and 180 min after loading. The symbols m and n denote the lines of network after deformation, as shown in Figs. 3 and 4. In these figures, the solid and dashed curves show the distributions of σ_m and σ_n on the surfaces on the die side ($n=0$) and punch side ($n=10$), respectively.

Fig. 14 shows the distribution of shear stress τ_{mn} on the contact surface between punch and strip or die and strip at 180 min after loading. In the figure, the solid or dashed curve shows the distribution on the surface of strip or punch and die. As shown in the figure, the magnitude of shear stress is far small in comparing with that of σ_m and σ_n shown in Figs. 12 and 13. The difference between solid and dashed curves may be attributed to the squeeze effect of an oil film lying on the contact surface. If so, it may be said that the locations where the stress σ_n attains to its extreme value must coincide with those of intersection of the solid and dashed curves expressing τ_{mn}. In the figure, such a condition is satisfied fairly well.

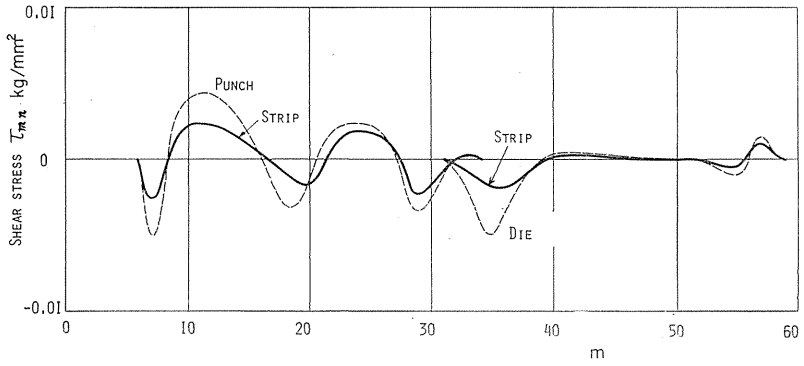

FIG. 14. Distribution of shear stress τ_{mn} on the contact surface at 180 min after loading.

6. Discussion and conclusion

The small triangles in Fig. 13 show the values of pressure σ_n on the contact surface obtained by photoelasticity on the punch or die side, and they agree well with the curve showing the corresponding value of pressure σ_n obtained by photo-rheological stress analysis on either contact surface of the strip. This shows that the condition of continuity of normal stress components of tools and strip on the contact surface is satisfied well.

As shown in Fig. 3, the strip is in the state of nearly line contact with punch or die at 2 min after loading. However, in Fig. 4 showing the state at 180 min after loading, the strip comes into contact with punch or die along whole surface except for the small region about the tip of punch.

In Fig. 12, the values of σ_m on both surfaces of the strip within the range of $m=20$ to 25 are nearly equal with each other. However, as shown on Section $m=24$ in Fig. 10, the distribution of this stress component is far from uniform one in the thickness direction.

As shown in Fig. 12, the maximum value of σ_m appears in the vicinity of $m=19$ on the surface of punch side or $m=26$ on the surface of die side. This is

nothing but the large tensile stress appearing on the free surface near the part of strip indented by another body[8)9)]. However, as shown in Fig. 13, the above mentioned features have disappeared and the absolute value of σ_m itself has been reduced at 180 min after loading.

As shown in Figs. 10 and 11, the stress state in each section varies remarkably due to the change of loading state with lapse of time. The chain line in Fig. 11 indicates the mean value of tensile stress, and the double dotted chain line shows the point of intersection of the chain line and the solid curve showing σ_m. In Sections $m=10$ and 50, the mean value of tensile stress is very small in comparing with the maximum value of σ_m, so the state is very near to that of the bending without tension. The dashed line in the middle of thickness shows the position of the neutral plane according to Hill's method[2)].

According to Hill[2)], when the strip is subjected to bending moment, the element lying on the outside of the neutral plane is compressed while that lying on the inside of the plane is extended radially. Moreover, the neutral plane itself approaches to the inner surface with the progress of bending. In the present experiment, the experimental value of relative movement in the thickness direction in each element on Sections $m=10$ and 50 measured at 180 min after loading is compared with the corresponding value obtained by Hill's procedure. In Figs. 15 (a) and (b), the solid and dashed curves show the relative movements of the elements obtained by experiment and the corresponding values obtained by Hill's procedure on Sections $m=10$ and 50, respectively, in which the relative movement away from the contact surface is expressed as positive. In these figures, though the relative movement on the opposite surface to the contact one is zero for the dashed curve because Hill's procedure does not consider the axial stretching, in the experimental result shown with the solid curve, since the element on the same surface moves towards the contact surface because of the slight reduction of thickness due to axial stretching, the relative movement near the opposite surface is shown as negative.

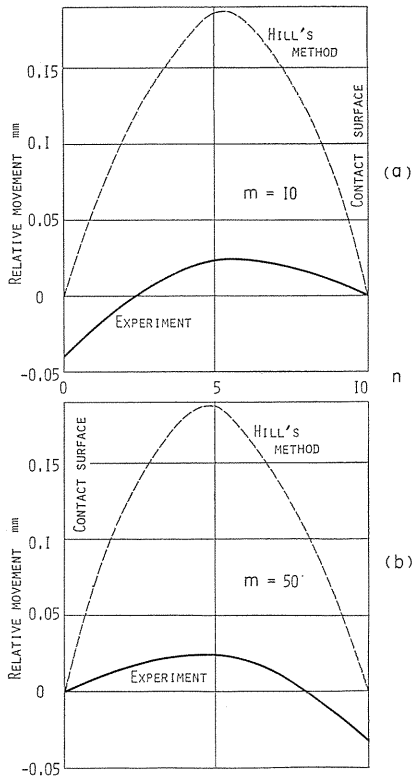

FIG. 15. Relative movements of the elements.
(a) $m=10$, (b) $m=50$.

References

1) O. Hoffman and G. Sachs: Introduction to the theory of plasticity for engineers, Mcgraw-Hill (1953), p. 266.

2) R. Hill: The mathematical theory of plasticity, Oxford press (1950), p. 287.
3) J. Gardiner: Trans. ASME, **79**-1 (1957), p. 1.
4) E. Rabinowicz: Trans. ASME, Ser. B, **85-1** (1963), p. 76.
5) D. F. Moore: Wear, 8-4 (1965), p. 245.
6) Y. Ohashi: J. Japan Soc. Tech. Plasti., **12**-129 (1971), (in Japanese).
7) Y. Ohashi and T. Nishitani: Int. J. Mech. Sci., **9** (1967), p. 359.
8) Y. Ohashi and T. Nishitani: Memoirs Facul. Eng., Nagoya Univ., **20**-1 (1968), p. 258.
9) Y. Ohashi, T. Nishitani and M. Tokuda: Int. J. Mech. Sci., **11** (1969), p. 1015.
10) Y. Ohashi, T. Nishitani and M. Ishida: J. Strain Analysis, **6**-4 (1971), p. 250.
11) J. W. Dally and W. E. Riley: Experimental stress analysis, Mcgraw-Hill (1965), p. 186.